N92-14090

THE IN-FLIGHT CALIBRATION OF THE HUBBLE SPACE TELESCOPE ATTITUDE SENSORS

Gary L. Welter
Computer Sciences Corporation
1100 West Street, Laurel MD 20707, U.S.A.

ABSTRACT

This paper presents a detailed review of the in-flight calibration of the Hubble Space Telescope attitude sensors. The review, which covers the period from the April 24, 1990, launch of the spacecraft until the time of this writing (June 1991), describes the calibrations required and accuracies achieved for the four principal attitude sensing systems on the spacecraft: the magnetometers, the fixed-head star trackers, the gyroscopes, and the fine guidance sensors (FGSs). In contrast to the other three sensor groups, the Hubble Telescope's FGSs are unique in the precision and performance levels being attempted; spacecraft control and astrometric research at the near-milliarcsecond level are the ultimate goals. FGS calibration accuracies at the 20-milliarcsecond level have already been achieved, and plans for new data acquisitions and reductions that should substantially improve these results are in progress. This paper presents a summary of the basic attributes of each of the four sensor groups with respect to its usage as an attitude measuring system, followed by a discussion of the calibration items of interest for that group. The calibration items are as follows: for the magnetometers, the corrections for the spacecraft's static and time-varying magnetic fields; for the fixed-head star trackers, their relative alignments and use in performing onboard attitude updates; for the gyroscopes, their scale factors, alignments, and drift rate biases; and for the FGSs, their magnifications, optical distortions, and alignments. The discussion covers the procedures used for each calibration, as well as the order of the calibrations within the general flow of orbital verification activities. It also includes a synopsis of current plans for the eventual calibration of the FGSs to achieve their near-milliarcsecond design accuracy. The conclusions include a table indicating the current and predicted ultimate accuracies for each of the calibration items.

I. INTRODUCTION

The ultimate scientific goals of the Hubble Space Telescope (HST) mission require relative pointing accuracy on the order of a few milliarcseconds for target objects within the telescope's 1/2-degree-diameter field-of-view (FOV). This high accuracy is to be achieved using the spacecraft's fine guidance sensors (FGSs), manufactured by Hughes Danbury Optical Systems, which allow the spacecraft to maintain pointing relative to a preselected set of guide stars. The milliarcsecond accuracy requirements for use of the FGSs dictate equally demanding accuracy requirements for their calibration. One of the purposes of this paper is to present an overview of the multistage procedure used for the calibration of the FGSs and the results obtained to date for that procedure. Another purpose is to describe the broader, sensor calibration context within which the calibration of the FGSs fits. The FGS FOVs are restricted to the outer 4-arcminute annulus of the telescope's full FOV. Because of the small size of the FGS FOVs, as well as the significant amount of time required to find guide stars using the FGSs, auxiliary systems are required for determining and controlling attitude at coarser levels. The principal auxiliary attitude determination sensors are the HST magnetic sensing system (MSS), manufactured by the Schonstedt Instrument Company; the fixed-head star trackers (FHSTs), manufactured by Ball Aerospace Systems Division; and the rate gyro assemblies (RGAs), manufactured by Allied Signal Aerospace Corporation. Use of these "auxiliary" systems, sometimes as the principal attitude sensing devices, has been common on many previous spacecraft (see Reference 1). This paper reports on the procedures used for the in-flight calibration of each of these auxiliary sensor groups for the HST mission. The description of the calibration of the FGSs follows that of the auxiliary sensors, paralleling the actual sequence of events followed during the orbital verification phase of the HST mission.

The data reduction and analysis algorithms used for the sensor calibration activities described in this paper have been implemented within the HST Payload Operations Control Center (POCC) Applications Software Support (PASS) system developed by Computer Sciences Corporation (CSC) under contract to the National Aeronautics and Space Administration / Goddard Space Flight Center (NASA/GSFC). The requirements for the PASS system, which continues to evolve, are documented in Reference 2. It is primarily from the author's perspective as a developer and user of the PASS system that this paper is written.

II. OVERVIEW OF HST AND ITS ATTITUDE SENSORS

Figure 1 shows the general layout of HST, including the locations of some of the important systems. The reader should note in particular the locations of the indicated magnetometer, magnetic torquer (MT), FHST, RGA, and FGS. (Companion instruments of each type are located symmetrically about the spacecraft.) The figure also indicates the locations of the optical telescope assembly (OTA), which comprises the primary and secondary mirrors and their mounting system, and one of the scientific instruments (SIs). In addition, it illustrates the standard reference frame of the spacecraft, with axes (V1,V2,V3), where V1 is along the primary viewing direction of the satellite, V2 is along the axis of the port side solar array, and V3 is along the upper high-gain antenna boom. [These are only approximate definitions; in actual operations the spacecraft axes are defined by the selected alignment matrix for FGS-2 (the FGS indicated in Figure 1). All other reference frames of interest are then measured relative to this fiducial frame.]

The four HST sensing systems of principal concern in this paper, the MSS, FHSTs, RGAs, and FGSs, are discussed in Sections IV, V, VI, and VII, respectively. Calibration of the sensors proceeds in essentially the same order in which they are discussed here. As an indication of the challenge involved with the full calibration, a few ballpark numbers are worth mentioning at this point. As noted in Section I, the design accuracy of the FGSs is a few milliarcseconds. The prelaunch errors in FGS calibration were estimated to be large enough to cause errors of up to 10 arcseconds in measured relative star separations. The relative mounting error between distinct sensors was estimated to be approximately 5 arcminutes. Finally, the error in HST attitude at the time of spacecraft release from the shuttle's remote manipulator system, as well as the attitude error during spacecraft recovery from a software sunpoint safemode situation, were estimated to be on the order of 6 degrees. HST's attitude determination and sensor calibration requirements thus range over a factor of nearly 10^7 in pointing resolution. Calibration of the MSS provides the capability to determine spacecraft attitudes to within approximately 3 degrees. This is sufficiently accurate to allow identification of stars observed by the FHSTs. Attitudes determined with the FHSTs prior to calibration of their relative alignments were good to approximately 10 arcminutes (the extra factor of 2 entering because of the geometry of the relative mountings of the trackers). Following alignment calibration, attitudes can be determined with FHST data to within approximately 20 arcseconds. Using FHST data to determine spacecraft attitudes, the RGAs can

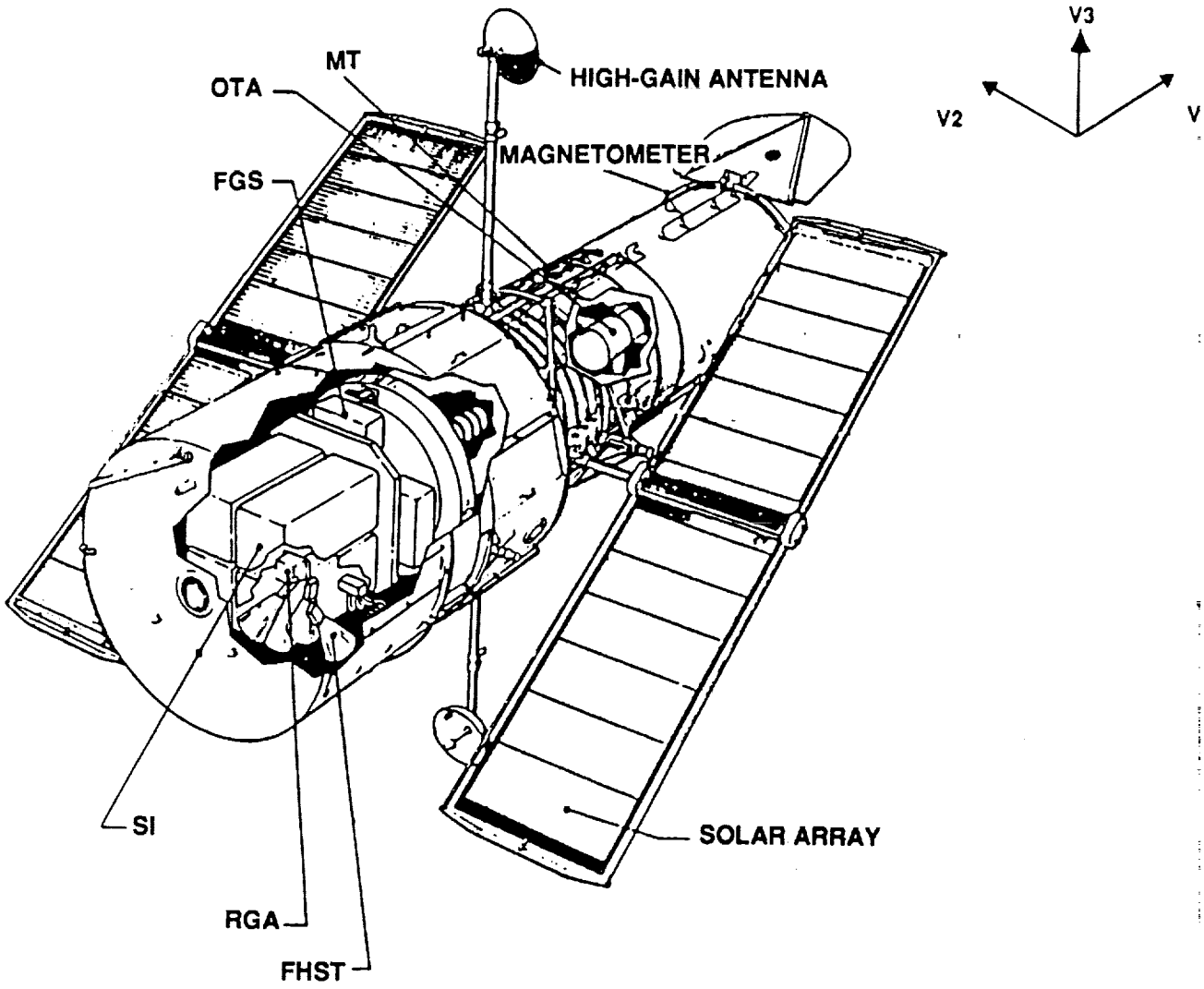

Figure 1. Hubble Space Telescope

be calibrated well enough to allow large-angle maneuvers with an accuracy of better than 60 arc-seconds. The accuracy of FHST attitudes also puts the system in the domain of the FGSs, at least after FGS calibration has proceeded through its initial stages. Detailed FGS calibration prepares the satellite to undertake its scientific objectives. A more detailed overview of each of these levels of calibration is given in the following sections.

III. GENERIC ATTITUDE DETERMINATION AND SENSOR ALIGNMENT

Much of the work described in this paper relies on the determination of either spacecraft attitude or sensor orientation based on a comparison of sensor-detected direction vectors (i.e., star direction vectors or geomagnetic field directions) to a known reference for those vectors. The mathematical problem is to find the attitude transformation matrix, **A**, that minimizes the loss function

$$L(\mathbf{A}) = 1/2 \sum [(| W_i - \mathbf{A} X_i | / \sigma_i)^2] \qquad (1)$$

where

W_i = i-th observation vector

X_i = associated reference vector [in geocentric inertial (GCI) coordinates]

σ_i = associated angular uncertainty

and the sum is over all observations. For the sensors discussed in this paper, X_i is obtained either from a star catalog (when FHST or FGS data are being used) or a geomagnetic field model (when MSS data are being used). Solving for the attitude matrix **A** requires a minimum input of two noncolinear observation vectors, with best results achieved for cases where substantial angular variation between vectors is involved. The algorithm used in PASS for the determination of the matrix **A** is one originally developed by P. Davenport and refined by M. Shuster. A complete discussion of the algorithm can be found in Reference 3.

The loss function of Equation 1 can be used as the basis of an algorithm for the determination of the relative alignments of two independent vector-direction sensors, or the relative attitude change of a given sensor over a period of time. Indeed, the PASS system uses this approach in certain of its algorithms. Another possible approach for the determination of a set of transformation matrices, $\{\mathbf{T}_1, \mathbf{T}_2, ..., \mathbf{T}_N\}$, that link a set of N sensors to a common reference frame is to minimize the loss function

$$L(\mathbf{T}_1, \mathbf{T}_2, ..., \mathbf{T}_N) = 1/2 \sum [(C_{W,(\mu i)(\nu j)} - C_{X,(\mu i)(\nu j)})^2 / (S_{(\mu i)(\nu j)})^2] \quad (2)$$

where

$C_{W,(\mu i)(\nu j)} = (W_{\mu i} \cdot W_{\nu j})$

$C_{X,(\mu i)(\nu j)} = (\mathbf{T}_\mu X_{\mu i} \cdot \mathbf{T}_\nu X_{\nu j})$

$W_{\mu i}, W_{\nu j}$ = i-th and j-th observation vectors in sensors μ and ν, respectively

$X_{\mu i}, X_{\nu j}$ = associated reference vectors

$(S_{(\mu i)(\nu j)})^2 = (\sigma_{\mu i}^2 + \sigma_{\nu j}^2) (W_{\mu i} \times W_{\nu j})^2$

$\sigma_{\mu i}, \sigma_{\nu j}$ = angular uncertainty for the i-th and j-th observations in sensors μ and ν, respectively

and the sum is performed over all pairs of unique observations between distinct sensors. (Note that $(S_{(\mu i)(\nu j)})^2$ is the variance associated with $C_{X,(\mu i)(\nu j)}$.) The PASS procedure for solving for the set $\{\mathbf{T}_1, \mathbf{T}_2, ..., \mathbf{T}_N\}$ in the case of relative FHST-to-FHST or FHST-to-FGS alignment determination is documented in Reference 2.

IV. CALIBRATION AND USE OF THE MAGNETOMETERS

The HST MSS consists of two magnetometers mounted on the outer hull of the satellite near the forward aperture. The magnetometers are designed to have a range of approximately -0.6 to +0.6 gauss, with a resolution of 0.0048 gauss per count. The MSS can be used to measure the local geomagnetic field in the spacecraft reference frame. These measurements, if taken over a sufficiently long period of time (i.e., at sufficiently many distinct positions in the spacecraft orbit) to

allow significant variation of the sampled geomagnetic field, can be used in conjunction with a geomagnetic field model (e.g., Reference 4) to determine the spacecraft attitude. Empirically it has been found that 20 minutes of MSS data allow determination of the attitude to within approximately 3 degrees, sufficient to allow attitude determination with the FHSTs.

The achievement of 3-degree attitude accuracy with MSS data requires some in-flight calibration of the MSS, part of which must be done before an accurate estimate of the spacecraft attitude has been determined. The most important in-flight calibrations of the MSS pertain to the magnetometers' response to the magnetic field generated by the spacecraft itself. This field may be divided into two parts: (1) a static bias produced by the magnetization of the spacecraft as a whole (including any intrinsic magnetometer bias) and (2) a time-varying field produced by the spacecraft's magnetic torquing system (MTS), which is part of HST's momentum management system. (The MTS field is used to couple the spacecraft to the Earth's magnetic field, which allows the dumping of excess spacecraft angular momentum to the Earth's field.) Both of these field components must be either eliminated or compensated for before application of the attitude determination algorithm will yield accurate results. The MTS-generated field can be removed by the deactivation of the MTS, a procedure that was used during the acquisition of MSS data shortly after HST's release from the shuttle's remote manipulator system. With all time variation of the measured magnetic field being due to motion of the spacecraft through the geomagnetic field, it is possible to determine the static spacecraft magnetic bias without knowledge of the spacecraft's attitude; the algorithm used by the PASS system for this initial bias determination is presented in Reference 5. The magnitude of HST's static field at the locations of the two magnetometers at the start of the mission was found to be roughly 0.020 gauss, with an uncertainty of 0.006 gauss. With the static bias determined, the MSS data were then reprocessed to provide an estimate of the spacecraft's attitude accurate to the aforementioned 3 degrees. This in turn allowed use of the FHSTs to commence.

Given an independent means of determining the attitude of the spacecraft (i.e., using the FHSTs), it is possible to calibrate the MSS for better estimates of its sensitivity to static bias and MTS-generated fields. The currently implemented algorithm for correcting MSS data for the effects of the MTS-generated magnetic fields is based on the MTS model used by the onboard computer for its momentum management computations. MTS field strengths at the locations of the magnetometers are estimated to be typically about 0.05 gauss. For the purposes of HST's momentum

management needs, it was found that the MTS field can be represented as a simple time-varying magnetic dipole at the center of the satellite. This approximation was incorporated into the ground-based attitude determination software to correct MSS data for the effects of the MTS field. In-flight calibration of the MSS to account for the two spacecraft field sources is calculable via the minimization of the loss function

$$L_\mu = \Sigma \left(B_{\mu i} - b_\mu - T_\mu D_i - A_i R_i \right)^2 \qquad (3)$$

where

$B_{\mu i}$ = magnetic field vector measured by magnetometer μ at time i

b_μ = static bias vector at magnetometer μ (to be solved for)

T_μ = MTS coupling matrix for magnetometer μ (to be solved for)

D_i = MTS dipole moment vector at time i

A_i = GCI-to-HST attitude transformation matrix at time i

R_i = geomagnetic reference field at HST's location at time i

The loss function used in PASS for the determination of b_μ and T_μ is actually somewhat more complicated than that of Equation 3 in that it also allows for an adjustment of the magnetometer alignment matrices. The details of the algorithm used to minimize the loss function are documented in Reference 2. A preliminary, "full" MSS calibration was performed a few months after launch. Approximately 600 data points, taken at 30 well-distributed attitudes and over the full range of MTS current readings (-2000 to + 2000 amperes · meters^2), were used in the calibration. The accuracy for the postcalibration correction for static and time-varying magnetic fields as sensed at the magnetometers was found to be approximately 0.005 gauss. Empirically it has been found that, for data taken within a few weeks of the calibration, use of the in-flight calibration parameters allows attitude determination with the MSS to within about 3 degrees even with the MTS active. In contrast, if in-flight calibration values for the static bias are applied, but prelaunch values for the MTS coupling matrix are used, the determined attitudes are accurate to only about 6 degrees. A subsequent review of the accuracy of MSS-derived attitudes has suggested a secular variation of the static bias. The details of this secular variation remain under investigation.

A refinement to the model for representing the MTS-generated field is being considered. The MTS consists of four magnetic torquer bars whose separations from each other are about one-third their separations from the magnetometers. For this reason it has been suggested that a better MTS model would use four dipoles, each centered at the location of one of the bars. When time permits, this enhancement to the representation of the MTS field may be incorporated into the PASS system.

V. CALIBRATION AND USE OF THE FIXED-HEAD STAR TRACKERS

The HST FHST system consists of three star cameras, each having an 8-degree-by-8-degree FOV and capable of detecting stars within the visual magnitude range of approximately 2 to 6 m_V. As indicated in Figure 1, the FHST FOVs are directed significantly away from the principal axis of the telescope. FHST-1 is mounted so as to have its boresight approximately along the -V3-axis. FHST-2 and FHST-3 are mounted so as to point downwards and backwards in the spacecraft reference frame. Their boresight direction-vectors are located within a plane rotated approximately 45 degrees about the V2-axis away from the V2/V3 plane, the individual boresight directions being 30 degrees to either side of the V1/V3 plane. The HST design imposes the operational restriction that only two FHSTs can be active simultaneously. The one-sigma accuracy of the HST star trackers is estimated to be approximately 11 arcseconds. This 11-arcsecond accuracy for a single FHST is obtained after distortion effects have been removed. FHST distortion is a function of position with the FOV, ambient temperature and magnetic field conditions within the tracker, and brightness of the observed star. Calibration of the FHSTs for distortion was performed on the ground, will not be repeated in orbit, and will not be further discussed in this paper.

The FHSTs operate in a number of modes, two of which are relevant to the discussions of this paper. The first, map mode, simply causes a given FHST to scan across its entire FOV and record all stars that it detects. When operating in map mode, the FHSTs are typically configured to have an observing rate of approximately one star every 20 seconds per active tracker. Ground-based attitude determination is performed using map mode data and the least-squares algorithm associated with Equation 1. It is by means of such ground-determined attitudes that the onboard computer's attitude knowledge is initialized (e.g., after spacecraft release from the shuttle or during spacecraft

recovery from a safemode situation). The accuracy of such computed attitudes was restricted at the beginning of the mission by the uncertainty in the relative alignments of the FHSTs, which were known only to about 5 arcminutes. An iterative algorithm using the loss function of Equation 2 is used by PASS to determine the relative alignments of the FHSTs; the details of the algorithm are presented in Reference 2. Because of the restriction that only two FHSTs can be active simultaneously, a minimum of three sets of data (one for each pair of trackers) is required to obtain a good alignment determination for the complete triad. The use of multiple data sets for each tracker pair is the standard procedure. Typically, from 5 to 10 fairly well-distributed stars are found in each tracker FOV during alignment calibration work. At 20 seconds per star, this implies an observing period of approximately 3 minutes to map the star fields for each pair of trackers. Proper alignment calibration therefore requires that the spacecraft gyroscopes have been sufficiently well calibrated to hold the spacecraft steady (or correct ground calculations) to significantly better than about 4 arcseconds per minute. Because the estimated prelaunch gyro bias uncertainty was approximately this value, iteration between gyroscope calibration and FHST alignment calibration at the beginning of the mission was required. Given the large number of star observations used in the tracker alignment procedure, statistical reduction of errors yields alignment accuracies a few times better than the 11-arcsecond accuracy level for a single observation. After alignment calibration is completed, it is the accuracy of the individual FHSTs coupled with the geometry of the tracker mountings, rather than the accuracy of the alignment determination, that sets a limit on the accuracy of the spacecraft attitudes that can be derived based on tracker data. Given N star measurements in each of two trackers with a separation angle of α between the trackers, the derived attitude would have a one-sigma "roll" uncertainty of $\sim \{ 11 / [(2N)^{1/2} \cdot \sin(\alpha/2)] \}$ arcseconds about the axis bisecting the chord connecting the trackers. Taking $N \sim 5$, this corresponds to about 7 arcseconds for the HST trackers.

The second mode of operation, update mode, uses one star in each FHST in operation. These data are used by the onboard computer to determine any adjustments to the spacecraft attitude required to reposition to the scheduled attitude. In practice, such attitude corrections are essentially always required after large vehicle maneuvers. The onboard algorithm for attitude error correction (details of which may be found in Reference 6) incorporates a simplifying approximation; it effectively assumes that the observed stars are near the FHST boresights. This approximation introduces an error on the order of $\beta \cdot [1 - \cos(\gamma)]$, where β is the true attitude error (i.e., deviation from desired

attitude), and γ is angular distance of the observed star from the center of the tracker. HST is currently operated with a restriction of 300 arcseconds on the value of β correctable by the onboard computer, whereas γ is restricted by the size of the FHST FOV to be less than about 5 degrees. This yields a maximum $\beta \cdot [1 - \cos(\gamma)]$ error of order 1 arcsecond. This is significantly smaller than the 20-arcsecond (one-sigma) error level inherent in FHST data having just one star per tracker (i.e., the onboard algorithm is effectively as accurate as a least-squares algorithm).

Although the update mode algorithm is, in principle, as accurate as a least-squares algorithm, significant difficulties in the use of update mode were encountered in actual operations. During the months immediately after launch, approximately 15 percent of scheduled FHST updates failed to properly correct the spacecraft attitude. The result was usually an inability to acquire FGS guide stars and a subsequent loss of scientific observations. Because of the criticality of successful FHST updates, a special analysis team was organized to study the causes of FHST update failures and to make recommendations for modifications to the ground and onboard algorithms so as to reduce the update failure rate. To a substantial extent, the difficulties with updates were found to have arisen as a consequence of (1) limitations of the update mode operation of the tracker hardware, (2) inexact specifications of FHST operating parameters, and (3) a few oversights in the original software package used for selection of FHST update stars. Update mode requires each of two FHSTs to find a preselected star in the FHST FOV. To this end, the FHST restricts its scanning operation to a 1.5-degree-by-1.5-degree reduced FOV (RFOV), accepting only stars brighter than a user-specified threshold. The center of the RFOV is not arbitrarily selectable, but rather is restricted to be one of a set of grid points spaced such that the set of all RFOVs covers the full FOV with overlap. Similarly, the star brightness threshold is not arbitrarily specifiable, but rather is restricted to one of four FHST response values corresponding to approximately 3, 4, 5, and 6 m_V. (Strictly speaking, the last "threshold" corresponds to all detectable stars.) It is one of the purposes of the PASS mission scheduling subsystem to select pairs of stars for FHST updates that are isolatable within FHST RFOV and brightness boundaries. The details of the algorithm for the selection of update pairs are beyond the scope of this paper; suffice it to say that the distribution of stars in brightness and position about the celestial sphere makes the problem an extremely nontrivial one. (Details may be found in Reference 2.) Careful tuning of input parameters is a necessity. Among those items studied and (where appropriate) tuned by the FHST anomaly analysis team are (1) the sensitivity response of each FHST as a function of FOV position, star

brightness, and star color, (2) the exact dimensions of the FHSTs' RFOVs, (3) the precision of the star brightness threshold limits, (4) reference star parameters (e.g. variability or incorrectly documented magnitude) for those stars used in unsuccessful updates, (5) command timing for FHST update executions, (6) FHST response error due to stray light (e.g., sunlight reflected from spacecraft components), (7) FHST plate scale response, (8) the possibility of enhancing an FHST's star isolation capability by means of an "error box" algorithm that will reject stars observed to be too far removed from the preselected position, and (9) the possibility of enhancing the probability of successfully updating the spacecraft attitude by scheduling multiple updates after major maneuvers. Modifications to ground or onboard systems have been made with respect to items 1 through 5; these modifications have already reduced the FHST update failure rate to approximately 4 percent. No significant correlation of update failures with spacecraft attitude or orbit position were found; this led to the dismissal of stray light (item 6) as a likely cause of update problems. Plate scale response (item 7) has been found to be nonnominal for FHST-3; starting in January 1991, that tracker has been minifying angular separations by about 0.25 percent. The cause of this anomalous scale behavior remains under investigation; correcting it will certainly prevent the recurrence of certain update difficulties that have recently been encountered. Recommendations for enhancements to onboard and ground software have been made with respect to items 8 and 9. Although improvement of system performance is anticipated upon implementation of each item, an exact determination of the degree of improvement -- particularly with respect to item 9 -- cannot be made at this time.

VI. CALIBRATION AND USE OF THE RATE GYRO ASSEMBLIES

HST's gyroscope system comprises three RGAs, each of which consists of two independently operable gyroscopes. The purpose of the RGAs is twofold: (1) to allow the spacecraft to remain at a fairly constant attitude while not using stars for guidance control and (2) to allow the spacecraft to perform large-angle slews with sufficient accuracy. In this context, "sufficient accuracy" means such that FHST updates can be performed after slews and thereby leave the spacecraft with an attitude good to within 60 arcseconds (three-sigma) of that intended. The basic design properties of the HST gyros are as follows. The mounting of the gyros is summarized via the matrix equation

$$
\begin{vmatrix} \omega_1 \\ \omega_2 \\ \omega_3 \\ \omega_4 \\ \omega_5 \\ \omega_6 \end{vmatrix} = \begin{vmatrix} -\sin(\alpha) & 0 & -\cos(\alpha) \\ -\sin(\alpha) & 0 & \cos(\alpha) \\ -\cos(\alpha)\sin(\beta) & -\cos(\alpha)\cos(\beta) & -\sin(\alpha) \\ \cos(\alpha)\sin(\beta) & \cos(\alpha)\cos(\beta) & -\sin(\alpha) \\ -\cos(\alpha)\sin(\beta) & \cos(\alpha)\cos(\beta) & -\sin(\alpha) \\ \cos(\alpha)\sin(\beta) & -\cos(\alpha)\cos(\beta) & -\sin(\alpha) \end{vmatrix} \begin{vmatrix} \Omega_1 \\ \Omega_2 \\ \Omega_3 \end{vmatrix}
$$

where ω_i represents a rotation about the i-th gyroscope, and Ω_j represents a rotation about spacecraft axis V_j. The design values for the angles α and β are 31.7 degrees and 43.5 degrees, respectively, α being a characterization of the mounting of the gyro with its RGA and β being a characterization of the RGAs' mounting on HST. The gyros can operate in two modes. The high-rate mode has a range of $\pm$ 1800 degrees per hour with a resolution of 7.5 milliarcseconds per 40-hertz sample. The low-rate mode has a range of $\pm$ 20 degrees per hour with a resolution of 0.125 milliarcsecond per 40-hertz sample. The three-sigma slew accuracy of the RGAs after calibration is estimated to be ~ 1 arcsecond per degree. The relative alignments of the HST gyroscopes is such that any three may be used to completely sample rotations of the spacecraft. The onboard control system is configured to use four gyros simultaneously, keeping the remaining two as backups. The active configuration immediately after launch was the set consisting of gyros 3, 4, 5, and 6. In December 1990, 8 months after launch, gyro 6 failed and was replaced in the control configuration by gyro 2. This configuration continues in use at the time of this writing.

The algorithm used within PASS for the calibration of an active gyro combination is presented in References 1 and 7. The basic thrust of the algorithm is to compare the responses produced by the gyros during a series of maneuvers with the known attitude changes across the maneuvers as determined using data from the FHSTs before and after each maneuver. (In principle, asymmetrically improved RGA calibrations can be achieved using attitudes determined with both FHST and FGS data. At present FGS data are not used.) If applied to a combination of three gyroscopes, the calibration procedure can yield information on the scale factor, alignment, and drift rate bias of the individual gyros. The one-sigma accuracy of the high-rate mode scale factor calibration is about 20 arcseconds per 90-degree maneuver, with roughly equal contributions coming from FHST attitude uncertainties and RGA nonlinearities. (The low-rate mode scale factors are not recalibrated

on orbit, but rather are assumed to be unchanged from their preflight values.) The alignment calibration is good to about 20 arcseconds, and the drift rate bias to about 5 arcseconds per hour for both high- and low-rate mode. The drift rate bias, for both high- and low-rate modes, has been found to vary at about 7 arcseconds per hour per day. As a consequence, the low-rate mode bias is recalibrated every 2 days and the high-rate mode bias every 7 days.

As indicated earlier, an asymmetric improvement in gyro calibration accuracy can, in principle, be achieved if FGS data are included along with the FHST data for attitude determination. This follows because the pitch/yaw accuracy of an attitude determined using FGS data is very good, restricted essentially by the accuracy of the ground-based catalog coordinates, which can be made good to better than an arcsecond. The HST astrometry team made a special effort to supply the HST orbital verification planning team with well-measured coordinates for stars in a set of 14 positions around the sky for use in this gyro calibration effort. Ultimately, at least as of this writing, the extreme difficulty in scheduling simultaneous FGS and FHST observations around the occultation patterns dictated by the calibration slews, coupled with the significant temporal variation of the drift rate bias, has led to a decision to restrict RGA calibration efforts to using only FHST-derived attitudes.

VII. CALIBRATION AND USE OF THE FINE GUIDANCE SENSORS

The heart of HST's pointing control system is the set of FGSs manufactured specifically for use on HST by Hughes Danbury Optical Systems. The FOVs of the FGSs are within the outer part of the full FOV of HST's primary optics. Each FGS FOV consists of an arc with an azimuthal range of 82 degrees and a radial range extending from approximately 10 arcminutes to 14 arcminutes relative to the primary optical axis of the telescope. Figure 2 illustrates the FOVs of the FGSs as they look out to the celestial sphere. The magnitude range for guide stars usable by the FGSs is approximately 9 to 16 m_V. The FGSs are designed to have an accuracy in determining relative star positions of approximately 3 milliarcseconds when fully calibrated (an accuracy not yet achieved at the time of this writing). The precision of the system follows from the design of an FGS as an amplitude interferometer using Koester's prisms combined with photomultiplier tubes. As with the

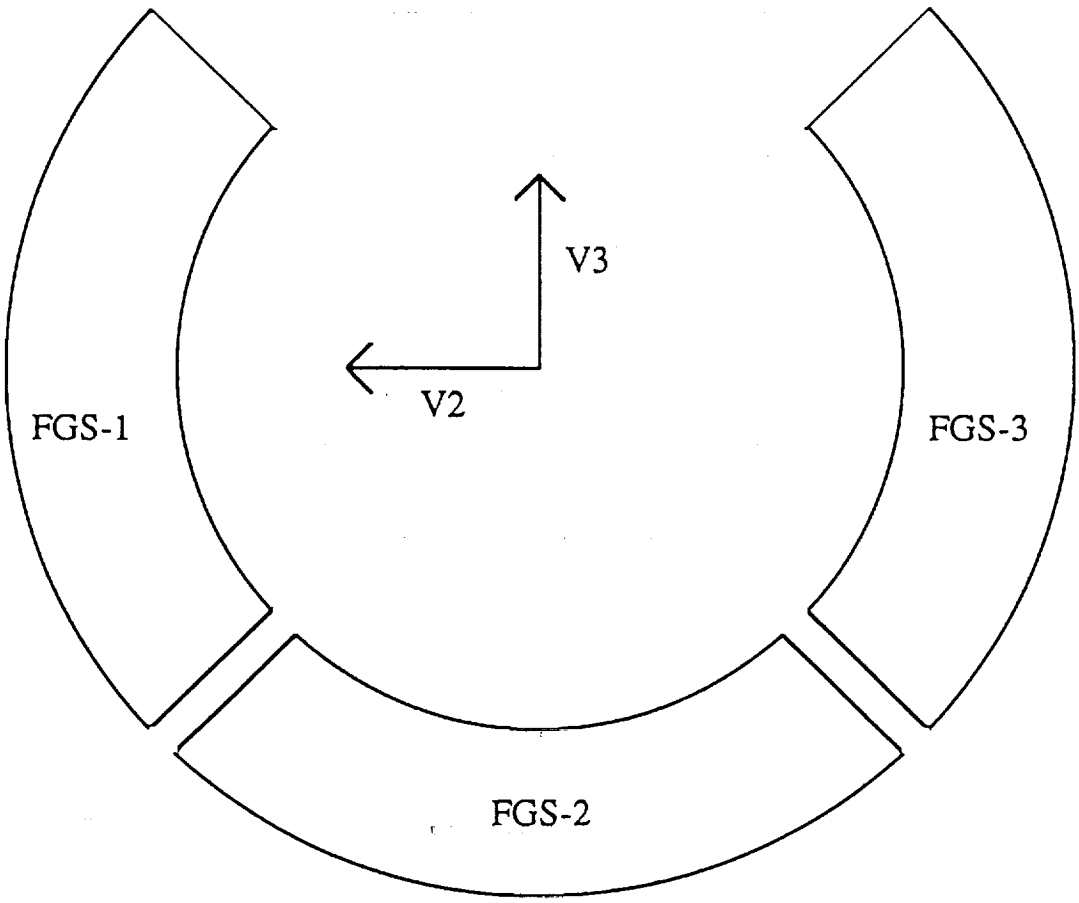

Figure 2. Fine Guidance Sensor Fields-of-View

FHSTs, an FGS can measure the position of only one star at a time. Each FGS has a 5-arcsecond-by-5-arcsecond instantaneous field of view (IFOV) that can be commanded to a selected position within the total FGS FOV. A star image falling within the inner 20 milliarcseconds of the IFOV will produce a significant interferometric signal. The FGS is said to be in fine lock when so measuring a star's direction. A second mode of FGS operation, coarse track mode, is also available. In this mode the center of the IFOV is commanded to nutate about the true star position in such a way that the edges of the IFOV cut across the image of the star in a symmetric pattern. The estimated design accuracy of determining star positions using coarse track mode is approximately 20 milliarcseconds. Because coarse track mode is less sensitive to spacecraft jitter than is fine lock mode, particularly for faint stars, it is expected that coarse track will regularly be used in observing situations in which extreme pointing precision is not required. Standard pointing control procedure during scientific observations is to use two of the FGSs to maintain guidance of the spacecraft, one for pitch/yaw stability and the other for roll stability. The remaining FGS is available for precise astrometric observations. This short description of the characteristics of the FGSs will suffice for the purposes of this paper. A more detailed description of the design and operation of the FGSs is available in Reference 8; indepth descriptions may be found in Reference 9.

The in-flight calibration of the FGSs consists of two major stages: external calibration and internal calibration. External calibration pertains to the alignment of the FGS triad to the rest of the spacecraft, whereas internal calibration pertains to the nonalignment-related parameters of the individual FGSs and the alignments of the individual FGSs relative to each other. External alignment is performed by gathering simultaneous data for FHSTs and FGSs and thereafter minimizing the loss function of Equation 2 while treating the FGSs as a single sensor. The most difficult aspect of the alignment effort pertained to the identification of the first stars observed with the FGSs. This initial alignment calibration of the FGS triad was done by pointing the telescope toward the open star cluster NGC 3532, commanding the guide FGSs to locate one star each in their FOVs for guidance, commanding the astrometry FGS to scan its FOV for as many stars as it could find within a specified magnitude range in the time available, and then attempting to match the pattern of stars found with stars in a reference catalog. Each FGS was used as the astrometry FGS three times during the exercise, with each astrometry scan covering a region of approximately 14 square arcminutes. In practice, this resulted in approximately six astrometry stars per scan. Practical

difficulties encountered during actual operations (certain of them related to the uncalibrated state of the FGSs at that time) led to modifications in the observing plans that ultimately made the star identification procedure and subsequent alignment calibration effort more laborious than anticipated. In particular, the lower limit on star brightness was set to 14 m_V, which is significantly fainter than the limit of the special NGC 3532 catalog provided by the HST astrometry team. This caused a certain degree of confusion and difficulty in identifying the observed star patterns. Approximately half of the observations were ultimately found in the original catalog. This allowed a preliminary determination of the relative alignments of the FGSs to the FHSTs -- preliminary in that most of the guide stars were unidentified and therefore the various baselines for FGS star separations were often no longer than about 6 arcminutes. The identification of the subset of observed stars, together with the FGS FOV coordinates for the whole set of observations, allowed the HST astrometry team to study specific regions on their NGC 3532 photographic plate and thereby provide catalog coordinates for the remaining stars. This enhancement allowed a final alignment calibration of the FGS triad to the FHSTs using FGS star separations that spanned the entire 28-arcminute-diameter FOV of the triad.

The internal calibration of the FGSs is divided into two phases. Phase 1 is intended to bring the calibration of the FGS system to an accuracy commensurate with ground-based astrometric observations. It does so by using such observations as reference points. Phase 2 goes beyond the limitations of ground-based astrometric work, the goal being to achieve the full near-milliarcsecond design capabilities of the FGS system. This second phase takes HST beyond any previously achieved ground or spacecraft calibration accuracies and requires extraordinary planning for both calibration programming and data acquisition. The basic goals of both phases of the on-orbit internal calibration of the FGSs are the determination of (1) the optical field angle distortion (OFAD) function for each FGS, (2) the magnification factor for each FGS, (3) the systematic offset between star positions determined in coarse track and those determined in fine lock for each FGS, and (4) the relative alignments of the FGSs. The details of the FGS calibration algorithms, particularly those for the phase 2 OFAD calibration, are of such complexity and demanding of such precision that a special analysis team was formed to analyze and develop the algorithm details. The team included representatives from CSC, GSFC, Hughes Danbury Optical Systems, Marshall Space Flight Center, and the University of Texas Astronomy Department. CSC personnel concurrently conducted an extensive feasibility and verification study of the FGS calibration algorithms as

part of their implementation. The details of the algorithms as implemented are documented in Reference 2; the results of the study are presented in Reference 10. An overview of each of the algorithms is presented below. The essential results of the study are that, based on certain assumed smoothness properties of the OFAD functions, the implemented algorithms are capable of determining the calibration parameters well enough to allow relative angular determinations to within a few milliarcseconds across each FGS FOV and between pairs of FGS FOVs. Independently, the astrometry teams at the University of Texas and Yale University have implemented versions of HST FGS calibration software for their own astrometric studies; these are being used for independent analysis of the FGS calibration data.

The algorithm used for OFAD calibration is a constrained two-dimensional least-squares algorithm based on the least-squares technique presented in Reference 11. The essential idea is to minimize a loss function, L, subject to certain constraints applied to the associated state vector. The loss function can be expressed (slightly nonrigorously) as

$$L = \Sigma \{ [W_{ij} - D(W_{ij},S) - A_j X_i]^2 / \sigma_{ij}^2 \} \quad (4)$$

where

W_{ij}	=	observation of star i in observation set j
$D(W_{ij},S)$	=	OFAD correction vector function
S	=	OFAD correction function parameter set (to be solved for)
A_j	=	attitude transformation matrix between attitude frame j and a selected standard reference frame (to be solved for)
X_i	=	"true" direction vector for star i in the standard reference frame (after correction for velocity aberration effects)
σ_{ij}	=	measurement uncertainty for observation of star i in set j (may include error associated with X_i)

and the summation is done over all stars and observation sets. For HST OFAD calibration, the correction function $D(W_{ij},S)$ has been parameterized as separate polynomials in the x and y Cartesian projections of W. The set S is therefore a set of polynomial coefficients. The phase 1

OFAD calibration procedure solves for a state vector $\{S, A_j\ (j=1,n)\}$, where n is the number of observation sets. The vector set $\{X_i\}$ is provided as a priori knowledge from ground-based observations. The ground-based observations need be accurate only differentially; any systematic errors in $\{X_i\}$ will be absorbed in the matrices $\{A_j\}$. The selected constraints, applied to the set S, are that the operator D should apply no net affine transformations to the vectors $\{W_{ij}\}$. Specifically, there should be no systematic shift in centroid location, rotation, or scale of $\{W_{ij}\}$. (Optionally, the constraints can be applied to an integration across the FGS FOV rather than the set of observations.) This calibration can, in principle, be performed using a single set of data (i.e., with each star observed only once). The phase 2 OFAD extends the phase 1 procedure so as to include $\{X_i\}$ as part of the state vector, thereby eliminating any errors associated with ground observations from the solution. Unlike the phase 1 calibration, that of phase 2 requires multiple observation sets and significant variation of the spacecraft attitude. It is by moving the various target stars through locally different distortion variation in the FGS FOV that the relative distortion across the entire FOV becomes observable at FGS accuracy levels.

The algorithm used for magnification calibration is substantially simpler than that used for OFAD calibration. Angular separations as imaged in the FGS detector space (hereafter "image space") are magnified by a factor of approximately 57.2 over their true (or "object space") values. In a zeroth order (i.e., small-angle) approximation, the magnification calibration could be performed simply by computing the ratio of the measured image space angular separation of two sources to the object space separation. The magnification, which works along radial arcs intersecting the optical axis, produces a sufficiently large image space FOV as to invalidate any small-angle approach. The following algorithm is therefore used for FGS magnification calibration. Let (ψ_i,ρ_i) be the image space polar coordinates for the i-th star observed, ρ_i being the "radial" angular separation from the optical axis, and ψ_i being the azimuthal distance from an arbitrary reference direction. The object space angular separation, Θ_{ij}, between two points with coordinates (ψ_i,ρ_i) and (ψ_j,ρ_j) is given by the spherical trigonometric relation (see Reference 12)

$$\cos(\Theta_{ij}) = \sin(\rho_i / M)\sin(\rho_j / M)\cos(\psi_i - \psi_j) + \cos(\rho_i / M)\cos(\rho_j / M) \quad (5)$$

where M is the magnification factor. Given an independent determination (e.g., from ground-based measurements) of the true angular separation, θ_{ij}, and an estimate, $M_{ij,n}$, for the magnification, an improved estimate for the magnification can be obtained using the relations

$$(M_{ij,n+1})^{-1} = (M_{ij,n})^{-1} - F(M_{ij,n}) / F'(M_{ij,n}) \quad (6)$$

$$F(M) = \cos(\Theta_{ij}) - \cos(\theta_{ij}) \quad (7)$$

where $F'(M)$ is the derivative of $F(M)$ with respect to M^{-1}. This process can be repeated until M_{ij}^{-1} converges to an acceptable accuracy. The full iteration can be repeated for all observation pairs within a given observation set. Finally, a weighted average over all such estimates of M^{-1} can be obtained using the equation

$$\langle M^{-1} \rangle = \Sigma [M_{ij}^{-1} (\theta_{ij} / \sigma_{ij})^2] / \Sigma [(\theta_{ij} / \sigma_{ij})^2] \quad (8)$$

where σ_{ij} is the root-mean-square uncertainty associated with the i-j pair, and the sum is over all observation pairs. The phase 1 magnification calibration can be performed using the same data set as the phase 1 OFAD calibration, with the θ_{ij} values being taken from ground-based observations. The phase 2 calibration requires a more accurate determination of θ_{ij}. The plan is to perform this calibration using observations of an asteroid moving across the FGS FOV and to obtain the required θ_{ij} estimates using high-precision numerical calculations of the asteroid ephemeris. Studies of asteroids suggest that variations of order 10 milliarcseconds in the separation of center-of-light and center-of-mass may result due to asteroid tumbling. Center-of-light variations will be compensated for by allowing θ_{ij} to be modeled in the form

$$\theta_{ij} = \theta_{i1} - \theta_{j1} \quad (9)$$

$$\theta_{i1} = \theta_{i1}(\text{center-of-mass}) + \alpha + \varepsilon \sin[\omega(t_i - t_1) + \phi] \quad (10)$$

where α, ε, ω, and ϕ are selected to give a best least-squares fit between Θ_{i1} and θ_{i1}, and t_i is the time of the i-th observation. (The model neglects center-of-light variation perpendicular to the direction of asteroid motion and asteroid motion curvature in the FOV.) Solutions for $\langle M^{-1} \rangle$ and $\{\alpha, \varepsilon, \omega, \phi\}$ are performed separately and iteratively.

The FGS-to-FGS alignment algorithm uses a two-part procedure. Part 1 establishes the angular separations between stars for every pair of stars in a selected reference set. During phase 1 of FGS calibration these angular separations are determined using ground-based observations. In contrast, during phase 2 the angular separations are determined using a single FGS in astrometry mode while the spacecraft is held at a constant attitude. With these angular separations specified, part 2 uses them to determine the relative alignments of two FGSs by means of an algorithm that is essentially equivalent to the minimization of Equation 2. Although there are no a priori restrictions as to which FGSs must be involved in the alignment procedure for the phase 1 calibration, phase 2 calibration requires that FGS-2 be used. This follows because the reference angular separations are restricted to being no greater than the maximum viewable by a single FGS at a fixed attitude; the minimum angular separation between FGS-1 and FGS-3 exceed this restriction. Optimal alignment results will be achieved if the FGS used for the determination of the reference angular separations during part 1 is positioned so as to give equal coverage to the star fields to be observed by the two FGSs during part 2; i.e., the spacecraft should be reoriented between parts 1 and 2 by means of a 45-degree roll about the V1-axis.

The algorithms implemented within PASS do not solve for the coarse-track-to-fine-lock (CT/FL) position offset. That such calibration would be required was not fully realized until shortly before HST's launch. One of the goals of the FGS calibration team has been to establish an appropriate parameterization for the bias. The dominant source of CT/FL offset is believed to be field stop misalignment within the FGS optics, which would show itself predominantly as a systematic offset throughout the FOV. Variation of the CT/FL offset as a function of field position may occur, a possible cause being optical vignetting near the edges of the FGS FOVs. Recent data has in fact shown that there are both systematic as well as field dependent components to the CT/FL offsets for all three FGSs.

To date, FGS calibration efforts have been essentially restricted to phase 1 calibration efforts. A catalog of ground-based star coordinates for the open cluster NGC 5617 has been provided by the Yale University astrometry team for this phase of calibration. The data reduction analysis for these observations, which were taken using the Mount Stromlo 26-inch refractor telescope, are described in Reference 13. The estimated one-sigma accuracy of the catalog is 30 milliarcseconds. Two sets

of data have been taken for the purpose of distortion and plate scale calibration, the time periods being the final week of December 1990 and the final week of May 1991. For each set, HST was commanded to make a series of astrometric observations of the target cluster. In what follows, "frame" will refer to the data taken in a single orbit, during which a single pair of guide stars were used in controlling the vehicle's attitude. The December observations consisted of five frames of data for each FGS, each frame consisting of approximately 17 stars. Each frame was taken at slightly adjusted telescope pointings, the adjustments being made as ±1-arcminute maneuvers in pitch and yaw. The May observations consisted of a set of 7 frames of roughly 15 stars apiece per FGS. Between frame adjustments by means of ±1-arcminute pitch and yaw maneuvers were also made, with the extra two frames being adjusted by means of ±15-degree roll maneuvers. The actual number of unique stars in each data set was approximately 25; however, not all stars in the set were observed in every frame. The combined optical distortion and magnification one-sigma residuals (i.e., the residuals between catalog star coordinates and FGS star coordinates after the latter have been corrected for distortion and magnification) for the December data reduction were found to be approximately 70 milliarcseconds. These errors were subsequently found to be best explainable as systematic color- and magnitude-dependent distortion effects in the catalog data. These systematic catalog errors have been corrected using the FGS data as a comparison. FGS calibration work with the new catalog produces solutions with residuals of approximately 35 milli-arcseconds. The calibration results demonstrated reasonable consistency between the true and design coefficients characterizing the FGS distortion curves. In contrast, the calibration results suggest strongly that the relative rotational offset between two optical elements in each of FGSs 2 and 3 differ significantly from their design values of zero. Specifically, for the benefit of readers familiar with References 8 and 9, the relative offset between the star selector A and B measurements has been found to be 0.57 degrees for FGS-2 and -0.63 degrees for FGS-3. These values are significantly larger than the design uncertainty for the offset angles; possible reasons for this discrepancy remain under investigation. The distortion and magnification calibrations were repeated for each FGS using the data taken in May. The calibration results show significant differences between the two calibration dates, particularaly with respect to magnification. The magnification factor was found to increase for all three FGSs, the fractional increases being $1.2 \cdot 10^{-4}$, $7.5 \cdot 10^{-5}$, and $2.4 \cdot 10^{-5}$ for FGSs 1, 2, and 3, respectively. For FGS-1, this corresponds to a 100 milliarcsecond change in relative star separation for stars 14 arcminutes apart. A small fraction of this change, about 13 milliarcseconds, may be accounted for as due to known differences in the primary to secondary mirror spacing; the bulk of the change is unexplained.

differences in the primary to secondary mirror spacing; the bulk of the change is unexplained. The May data set was specifically designed to allow for a determination of the CT/FL offset. Each star in the astrometric FGS was observed for 30 seconds in coarse track prior to the transition to fine lock mode. This provided approximately 100 points distributed throughout each FGS FOV from which CT/FL offset could be determined. Analysis of the data indicates that the offset for each FGS is well represented by a linear model. The magnitude of the constant component of the offset ranges between 0.2 and 0.8 arcseconds for the three FGSs, while the field dependent component introduces offset changes of approximately 80 milliarcseconds across the 18-arcminute range of an individual FGS. The accuracy of the CT/FL offset correction is estimated to be approximately 5 milliarcseconds, although significant and systematic departures from the fit were observed for certain individual stars (i.e., the offset can be dependent on specific star properties).

Data specifically for phase 1 FGS relative alignment determination were also taken during the December observing period. The data consist of 17 frames of observations, each frame consisting of approximately 10 star observations in FGS-2 (used in astrometry mode) and one guide star in each of the other FGSs. Because of operational difficulties (e.g., the then unresolved solar array jitter problem), the data were taken with the guide FGSs (1 and 3) using coarse track mode. The locations of the stars within the FGS FOVs were selected so as to provide complete coverage when the data sets are combined. The data were processed, and corrections within each FGS for distortion, magnification, and CT/FL offset were applied. Relative FGS-to-FGS alignment calibrations were then performed. The postcalibration one-sigma residuals for the difference between measured and reference star separations between FGSs were found to be approximately 35 milliarcseconds, i.e., basically consistent with the estimated accuracy of the reference catalog. The implied accuracy for the alignment calibration is about 10 milliarcseconds. In order to verify these alignment calibrations, the May FGS 2 distortion data acquisitions were specifically designed with guide star distributions appropriate for an FGS-to-FGS alignment determination. These alignment results produced one-sigma residuals of approximately 54 milliarcseconds, with an implied alignment accuracy of about 20 milliarcseconds. Unexpectedly, the alignment solutions for the May data differed significantly from those for the December data, the differences being approximately 200 milliarcseconds. A third FGS data set appropriate for alignment determination was available from the end of January, 1991. These data also produced internally self-consistent alignment solutions with one-sigma residuals of about 50 milliarcsecond and accuracy of about

20 milliarcseconds. The January alignments are about 100 milliarcseconds different from either of the other two. At this point we have no physical explanation for the variations in the alignment solutions; the cause of the variability remains under investigation.

The two data sets accumulated for each FGS for phase 1 OFAD/magnification analysis have allowed a restricted amount of phase 2 OFAD processing. This admittedly very preliminary analysis has resulted in OFAD solutions with one-sigma residuals on the order of 7 to 10 milliarcseconds. Comparison of these phase 2 solutions with the phase 1 results indicates that the phase 2 software package is more robust than originally expected, and that reasonably accurate results for OFAD calibration can be obtained (at least for the central region of an FGS FOV) with as few as five frames of data. The ultimate OFAD phase 2 analysis will require approximately five times as much data for at least one of the FGSs. (Phase 1 OFAD processing can thereafter be applied to the other two FGSs using reference data from their well-calibrated sibling, thereby achieving full accuracy at a phase 2 level for all three FGSs.) Current plans place full phase 2 FGS calibrations no earlier than the last 2 months of 1991.

VIII. OPTICS CALIBRATION AND SCIENTIFIC INSTRUMENT ALIGNMENT

Two major calibration activities closely related to the calibration of the attitude sensors are not covered by this paper: the optics calibration and the calibration of the alignments of the apertures of the SIs. The optics calibration consists of the measurements and analysis performed in connection with the adjustment of the relative positions of the secondary and primary mirrors. It touches upon the topic of this paper in that the performance of the FGSs and their effective alignments relative to the other HST attitude sensors are functions of the relative configuration of the two mirrors. Adjustments to the tilt or decenter of the secondary mirror therefore necessitate recalibrations of the relative alignments of the other sensors to the FGSs. (In practice, only the FHST and RGA alignment matrices need respecification.) It was within the context of performing an optical calibration that representatives of Hughes Danbury Optical Systems (the mirror manufacturer) discovered the spherical aberration of the primary mirror. Because the FGSs are afocal systems, the manufacturer believes that the spherical aberration of HST's primary mirror will not significantly degrade the accuracy of the FGSs.

The aperture directions of the various SIs are located interior to the annulus of the FGS FOVs. Operationally, the SI aperture alignments are measured relative to a reference frame defined by the FGSs. The alignment calibration for any given SI is performed by taking simultaneous measurements with the SI and at least two of the FGSs, then comparing these measurements with accurate astrometric coordinates for the observed stars. This procedure clearly places a limit on the accuracy obtainable for the determined SI aperture direction; i.e., the alignment accuracy can be no better than the calibration accuracy of the FGSs. Because the ground system does not currently correct for the CT/FL offset, the SI aperture alignment accuracy is thus currently restricted by the operational FGS accuracy of about 0.8 arcsecond imposed by the uncompensated CT/FL offset in FGS 2. As the effective FGS accuracies improve, through both software upgrades to the operational system and actual improvements in the FGS calibration, operational improvements in the pointing of the SIs will result.

IX. SUMMARY

This paper has presented a review of the calibration algorithms and accuracies for the four principal attitude determination sensing systems aboard HST. Table 1 summarizes the current and ultimately expected accuracies for each of the calibration items discussed. Final calibration accuracy has essentially been achieved for the MSS, the FHSTs, and the RGAs; significant progress has been made in the calibration of the FGSs. Significant work continues with respect to tuning and enhancing the FHST update capability. Regular recalibration of the RGA drift rate bias is required because of its temporal variation. Periodic recalibration of the FHST and RGA alignments is required because of redefinitions of the spacecraft reference frame that result from (1) improved FGS calibration and (2) adjustments to the tilt or decenter of the secondary mirror. Significant progress has been made in the calibration of the FGSs, accuracies on the order of 10 to 20 milliarcseconds seem obtainable for a data set localized in time. An unexplained variation of the FGS magnifications and relative alignments, with effects on the order of a few hundred milliarcseconds, has been observed; this variation remains under investigation. Plans are being made for the acquisition of data designed for FGS calibrations accurate to the level of a few milliarcseconds.

Table 1. Attitude Sensor Calibration Accuracies

Sensor	Calibration Item	Current Accuracy	Expected Accuracy	Typical Value	Units
MSS	Static bias	~ 0.004	~ 0.004	~ 0.02	Gauss
	MTS coupling	~ 0.004	~ 0.004	~ 0.05	Gauss
FHST	Distortion	~ 11	~ 11	~ 60	Arcseconds
	Alignments	~ 4	~ 4	——	Arcseconds
RGA	Alignment (to FHSTs)	~ 30	~ 30	——	Arcseconds
	Scale factor (high-rate mode)	~ 0.4	~ 0.4	——	Arcseconds per degree
	Drift rate bias	~ 5	~ 5	~ 10000	Arcseconds per hour
	Bias change rate (high- and low-rate modes)	~ 4	~ 4	~ 7	Arcseconds per hour per day
FGS	Alignment (to FHSTs)	~ 10	~ 10	——	Arcseconds
	Distortion / (Magnification)	~ 0.010	~ 0.003	~ 5 (57.2)	Arcseconds (unitless)
	Alignment to FGSs	~ 0.015	~ 0.006	——	Arcseconds
	CT/FL offset	~ 0.010	~ 0.010	~ 0.5	Arcseconds
	Unexplained Variation			~ 0.2	Arcseconds

X. CALIBRATION TEAMS AND SUPPORTING ORGANIZATIONS

The following persons and organizations have been closely involved with HST sensor data analysis and calibration during the first year of the HST mission. The MSS / FHST / RGA data analysis team for the first few months of orbital verification consisted of John Boia[c], William Collier[c], Martin Gakenheimer[a], Edward Kimmer[a], Matthew Nadelman[c], Cherie Schultz[c], and Gary Welter (superscripts refer to organization affiliation; see list below). Responsibility for the periodic recalibration of these sensors has been turned over to the PASS operations contractor -- primarily Messrs. Gakenheimer and Kimmer, with most of the MSS calibration analysis being performed by Sidney Broude[a]. Individuals participating in the analysis of FHST update anomalies included Michael Brunofski[a], W. Collier, Paul Davenport[c], Larry Dunham[g], M. Gakenheimer, Theresa Gaston[g], Kevin Grady[d], Lou Hallock[d], Joseph Hennessy[d], Jeffery Karl[c], E. Kimmer, Raymond Kutina[c], Robert McCutcheon[c], M. Nadelman, William Ochs[d], Thomas Pfarr[c], Milton Phenneger[c], G. Welter, and Michael Wright[d]. NGC 3532 catalog star coordinates for the initial FGS alignment calibration were provided by George Benedict[k], Otto Franz[f], Lawrence Fredrick[l], Darrell Story[k], and Lawrence Wasserman[f]. The FGS calibration team consists of Linda Abramowicz-Reed[e], William Brady[e], Todd Burr[e], Roger Doxsey[j], Terrence Girard[m], Arun Guha[b], L. Hallock, William Jefferys[k], E. Kimmer, Young-Wook Lee[m], Bruce Lowenberg[e], Olivia Lupie[cj], William Van Altena[m], Qiangguo Wang[k], G. Welter, and Robert Zarba[e]. Numerous other individuals from many organizations provided extensive support for the activities described in this paper. These organizations include

a. Allied Signal Aerospace Corporation
b. AKG, Incorporated
c. Computer Sciences Corporation
d. Goddard Space Flight Center
e. Hughes Danbury Optical Systems
f. Lowel Observatory
g. Jackson and Tull
h. Lockheed Missiles and Space Company
i. Marshall Space Flight Center
j. Space Telescope Science Institute
k. The University of Texas Astronomy Department
l. The University of Virginia Astronomy Department
m. Yale University Astronomy Department

Many other individuals were involved with activities in prelaunch preparation for the calibration of the HST attitude sensors. Of particular note for their support in this area are Paul Davenport, whose analytic insights provided the basis for, or extensions of, many of the algorithms in the PASS system; Gerald Abshire[c], who coordinated the software development effort for the original implementation of most of the PASS sensor calibration algorithms; and Robert Coulter[i], who coordinated the intricate prelaunch scheduling of the early orbital verification activities. The calibration of HST will be an ongoing effort, with varying degrees of intensity, throughout the lifetime of the telescope. It is, and will continue to be, an interesting and stimulating intellectual challenge.

The work reported in this article was supported in part by NASA contract NAS-5-31500, which enables CSC to provide general systems engineering and analysis support to NASA/GSFC, including specific support for the HST mission.

REFERENCES

1. J. Wertz (ed.), Spacecraft Attitude Determination and Control, Dordrecht, Holland: D. Reidel Publishing Company, 1978

2. Computer Sciences Corporation, CSC/TM-82/6045, Space Telescope POCC Applications Software Support (PASS) Requirements Specification (Revision E), L. Hallock et al., September 1987

3. M. Shuster and S. Oh, *Three-Axis Attitude Determination from Vector Observations*, Journal of Guidance and Control, January 1981, vol. 4, no. 1, p. 70

4. National Space Science Data Center, Goddard Space Flight Center, Code 633.4, *International Geomagnetic Reference Field Revision 1987*

5. P. Davenport, W. Rumpl, and G. Welter, *In-flight Determination of Spacecraft Magnetic Bias Independent of Attitude*, GSFC Flight Mechanics / Estimation Theory Symposium, May 1988

6. Computer Sciences Corporation, CSC/TM-88/6103. Hubble Space Telescope (HST) Flight Software Examination for the Pointing Control Subsystem (PCS), L. Hallock, March 1990

7. P. Davenport and G. Welter, *Algorithm for In-flight Gyroscope Calibration*, GSFC Flight Mechanics / Estimation Theory Symposium, May 1988

8. A. Bradley, L. Abramowicz-Reed, D. Story, G. Benedict, and W. Jefferys, *The Flight Hardware and Ground System for Hubble Space Telescope Astrometry*, Publications of the Astronomical Society of the Pacific, 1991, vol. 103, p. 317

9. Marshall Space Flight Center, SMO-1040, Hubble Space Telescope Astrometry Operations Handbook, March 1987

10. K. Luchetti, G. Abshire, L. Hallock, and R. McCutcheon, *The Optical Field Angle Distortion Calibration Feasibility Study for the Hubble Space Telescope Fine Guidance Sensors*, GSFC Flight Mechanics / Estimation Theory Symposium, May 1988

11. W. Jefferys, *On the Method of Least Squares*, The Astronomical Journal, February 1980, vol. 85, no. 2, p. 177

12. W. Smart, Text-Book on Spherical Astronomy. Cambridge, England: Cambridge University Press, 1971

13. T. Girard, C. Heisler, Y.-W. Lee, C. Lopez, W. van Altena, and P. Ianna, *Astrometric Calibration Regions with Proper Motion Membership Estimates in the Open Clusters NGC 188 and NGC 5617,* Poster Presentation at the January 1990 Meeting of the American Astronomical Society held in Washington D.C.

FLIGHT MECHANICS/ESTIMATION THEORY SYMPOSIUM

MAY 21-23, 1991

SESSION 5